Supporting Information

Proton conduction in sulfonated organic-inorganic hybrid monoliths with hierarchical pore structure

Martin von der Lehr,[§] Christopher F. Seidler,[†] Dereje H. Taffa,[†] Michael Wark,[†] Bernd M. Smarsly,[§] Roland Marschall[§]*

§Institute of Physical Chemistry, Justus-Liebig-University Giessen, 35392 Giessen, Germany

†Institute of Chemistry, Carl von Ossietzky University Oldenburg, 26129 Oldenburg, Germany.

*Email: Roland.marschall@phys.chemie.uni-giessen.de

Results

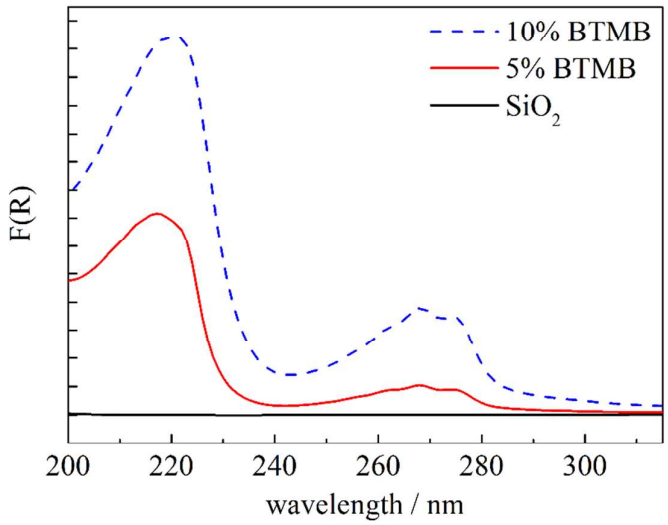

Figure S1. Absorption measurements of pure SiO_2 compared to unsulfonated hybrid monoliths containing 5 or 10% BTMB.

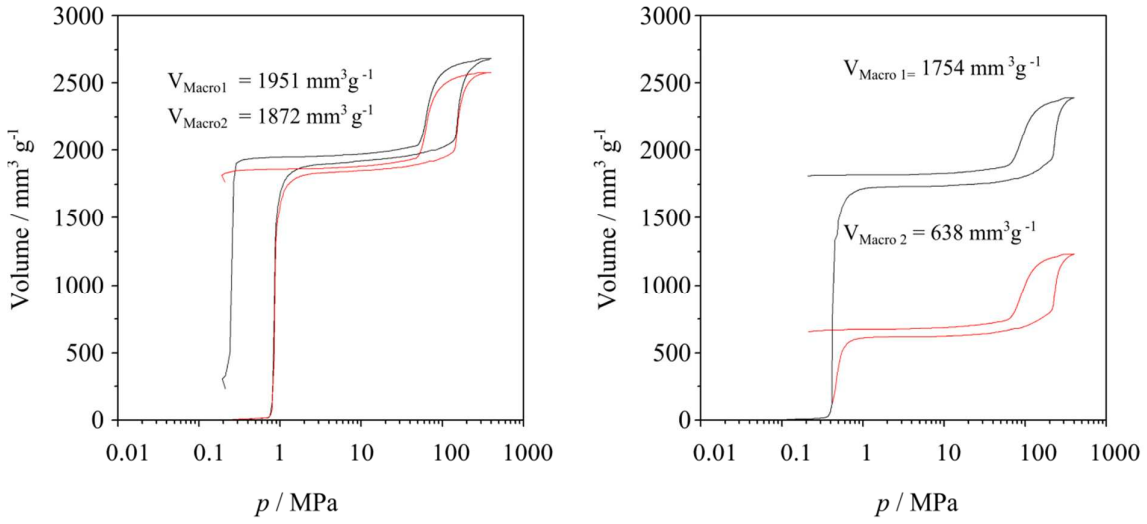

Figure S2. Mercury intrusion/extrusion curves of two consecutive cycle runs (1st run: black line, 2nd run: red line) of the samples HTT 368/27 containing 5% BTMB (left) and 10% BTMB (right), respectively

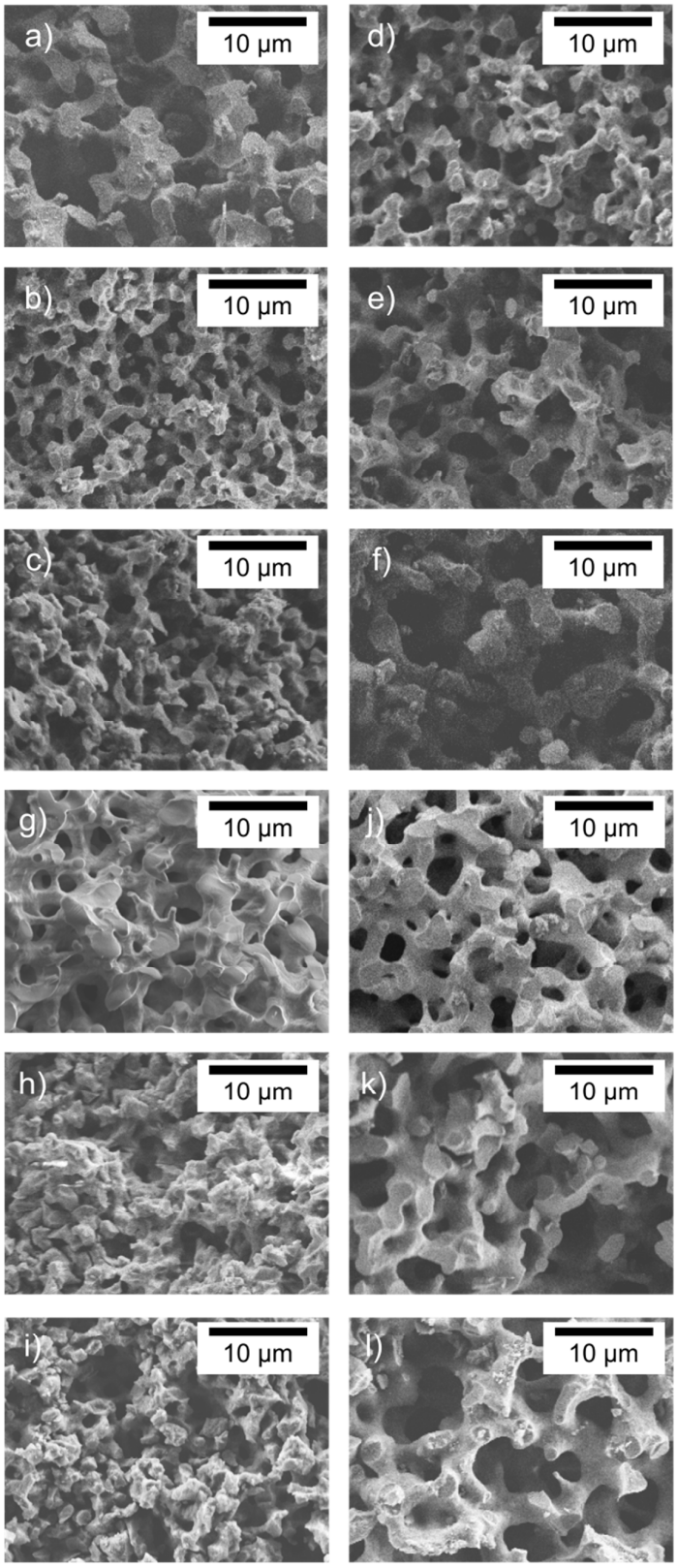

Figure S3. SEM images of solvothermally treated samples before sulfonation, a) 5% BTMB HTT 353/15, b) 5% BTMB HTT 353/27, c) 5% BTMB HTT 368/27, d) 10% BTMB HTT 353/15, e) 10% BTMB HTT 353/27, f) 10% BTMB HTT 368/27 and after sulfonation g) 5% BTMB HTT 353/15, h)

5% BTMB HTT 353/27, i) 5% BTMB HTT 368/27, j) 10% BTMB HTT 353/15, k) 10% BTMB HTT 353/27, l) 10% BTMB HTT 368/27.

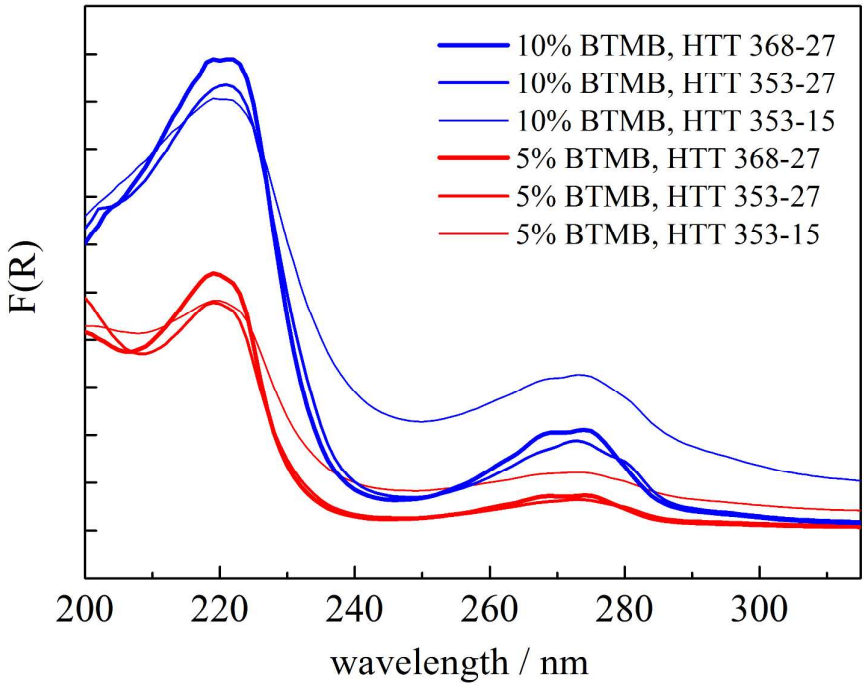

Figure S4. Absorption spectra of sulfonated hybrid monoliths.

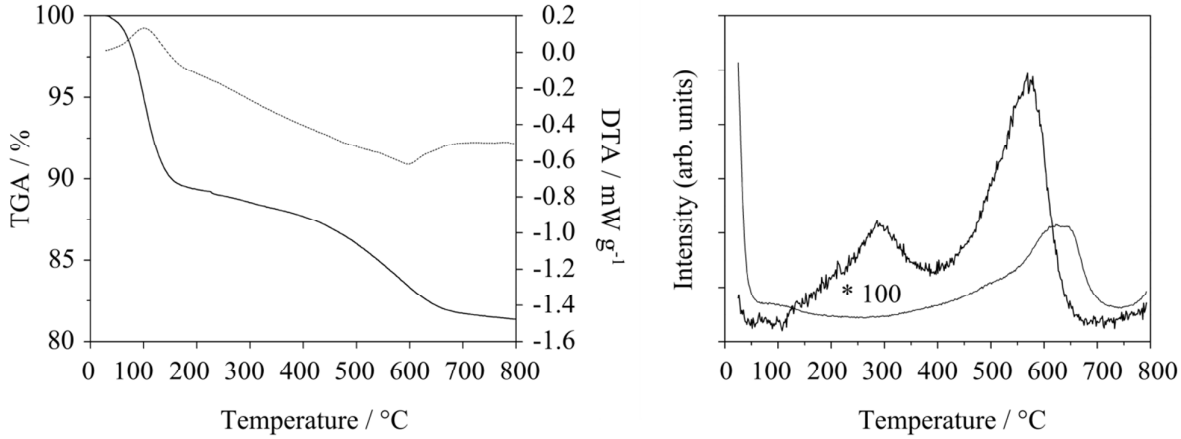

Figure S5. Left: TGA and DTA (dashed line) of monolithic hybrid (HTT 353/15) containing 5% BTMB; Right: according TG-MS traces with detected m/z = 44 (CO_2) and m/z = 64 (SO_2) as annealing products from the decomposition of the sulfonated aromatic moiety.

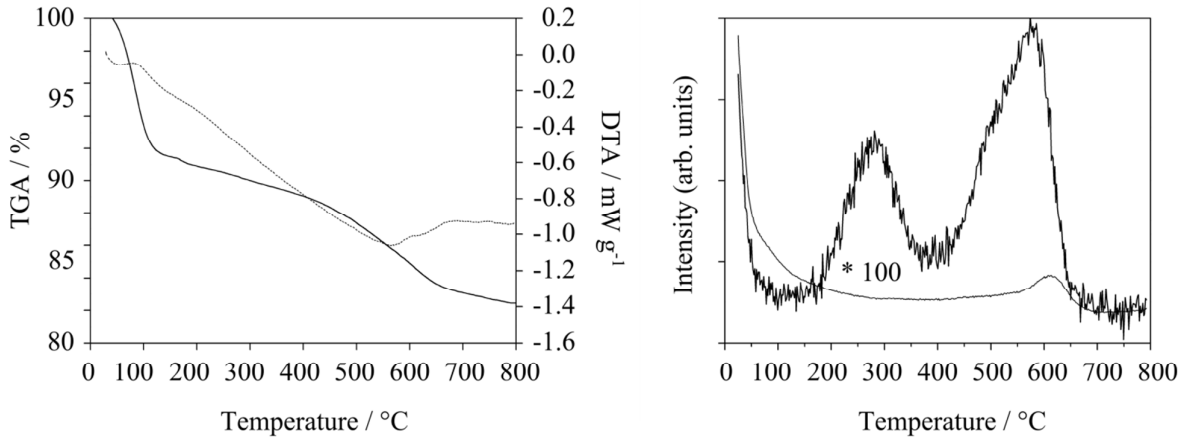

Figure S6. Left: TGA and DTA (dashed line) of monolithic hybrid (HTT 353/27) containing 5% BTMB; Right: according TG-MS traces with detected m/z = 44 (CO_2) and m/z = 64 (SO_2) as annealing products from the decomposition of the sulfonated aromatic moiety.

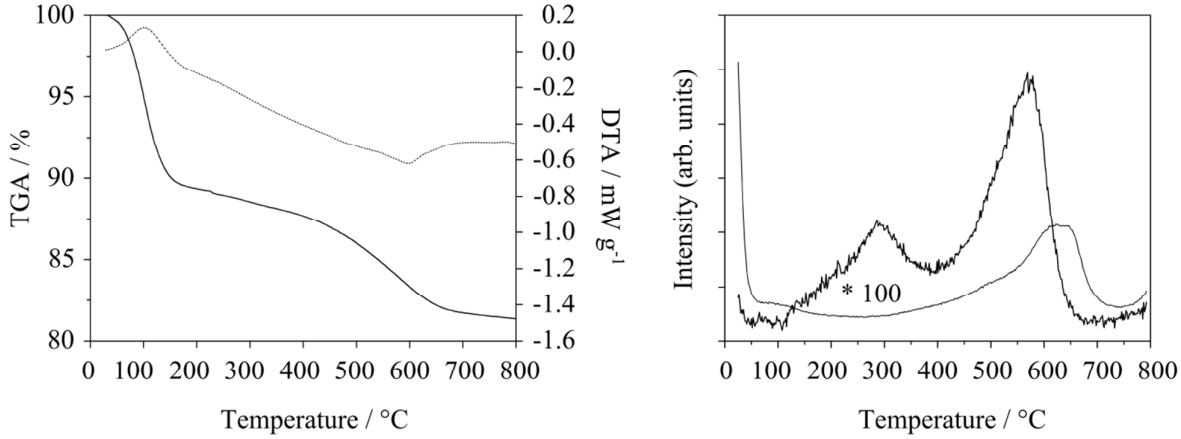

Figure S7. Left: TGA and DTA (dashed line) of monolithic hybrid (HTT 368/27) containing 5% BTMB; Right: according TG-MS traces with detected m/z = 44 (CO_2) and m/z = 64 (SO_2) as annealing products from the decomposition of the sulfonated aromatic moiety.

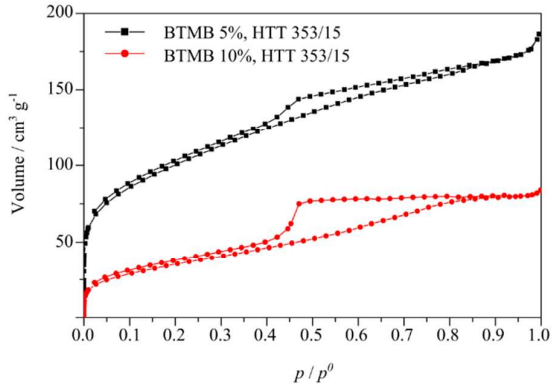

Figure S8. Low pressure N_2 physisorption isotherms from micropore analysis for hybrid monolith samples HTT 353/15 containing 5% BTMB (black symbols) and 10% BTMB (red symbols) after solvothermal treatment and sulfonation.

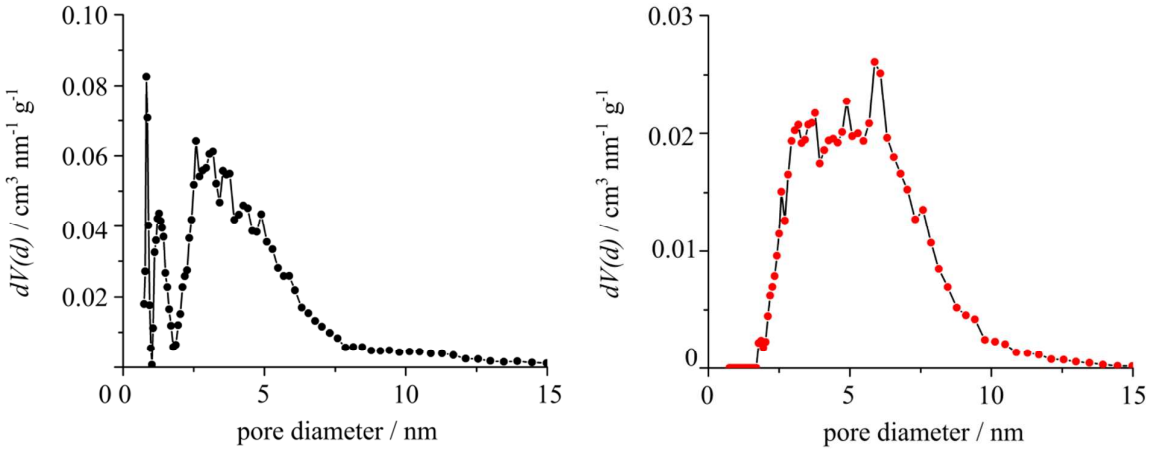

Figure S9. Pore size distribution from low pressure micropore analyses via NLDFT adsorption branch model for hybrid monolith samples HTT 353/15 containing 5% BTMB (left) and 10% BTMB (right) after solvothermal treatment and sulfonation.

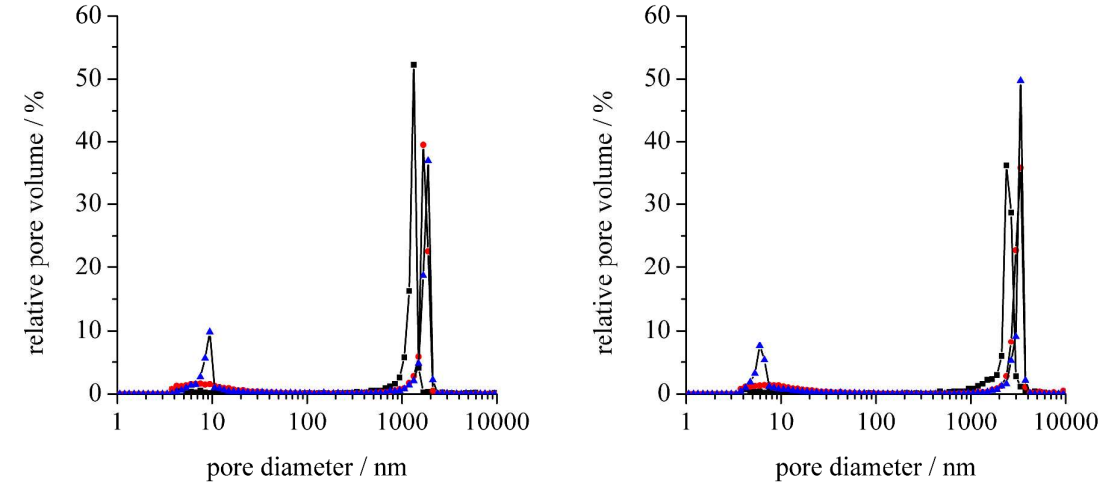

Figure S10. Mercury intrusion porosimetry for sulfonated meso-macroporous hybrid monoliths containing 5% BTMB (left) and 10% BTMB (right) after solvothermal treatment at (■) HTT 353/15, (●) HTT 353/27, (▲) HTT 368/27.

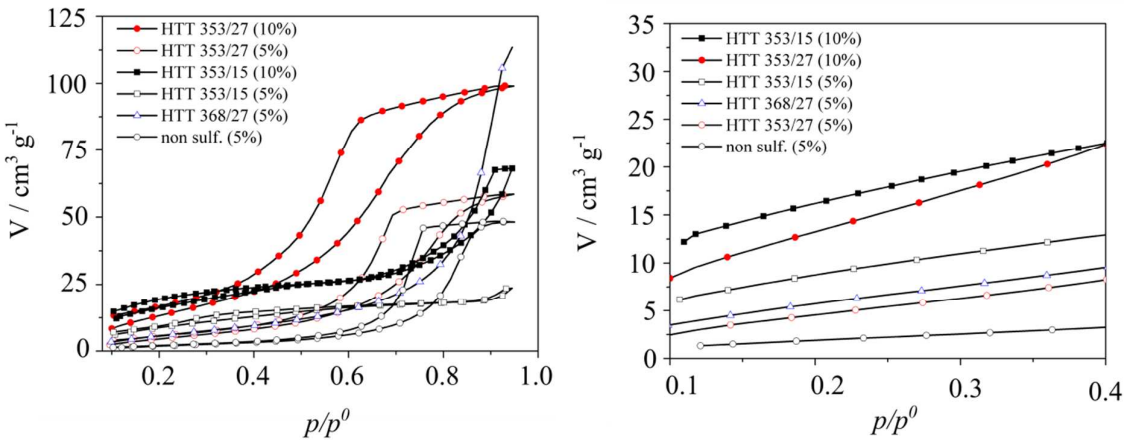

Figure S11. Water sorption isotherms of sulfonated and non-sulfonated monolithic hybrid materials performed at 298 K; full isotherms (left) and zoom in of adsorption branches at lower relative pressures (right).

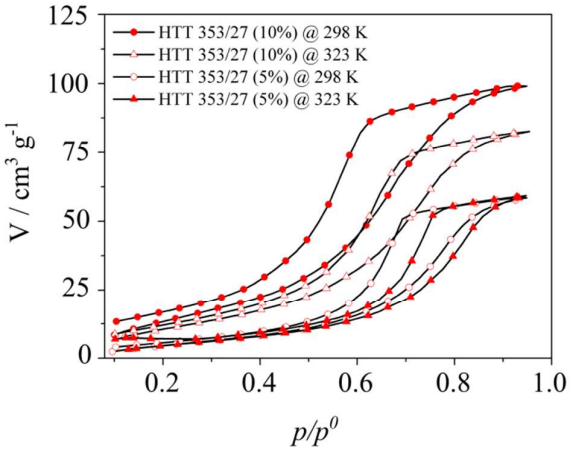

Figure S12. Water sorption isotherms of sulfonated monolithic hybrid materials HTT 353/27 at different temperatures.

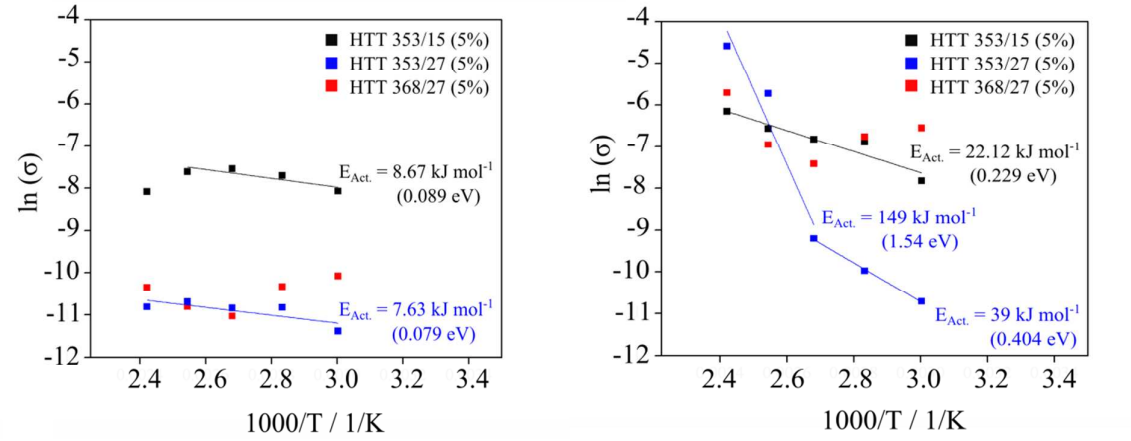

Figure S13. Arrhenius plots with activation energies of sulfonated hybrid monoliths containing 5% BTMB at 50% relative humidity (left) and 100% relative humidity (right).

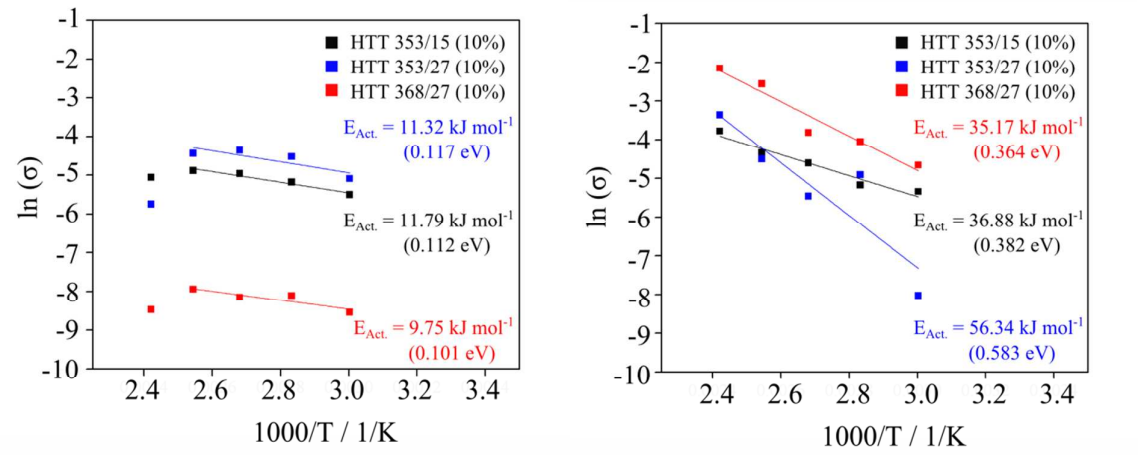

Figure S14. Arrhenius plots with activation energies of sulfonated hybrid monoliths containing 10% BTMB at 50% relative humidity (left) and 100% relative humidity (right).

Table S1. Results from CHNS elemental analyses

Sample name	C (%)	H (%)	N (%)	S (%)	S (mmol g^{-1})
TMOS/BTMB (95/5), SO_3H HTT 353/15	2.13	1.85	0.01	0.89	0.218
TMOS/BTMB (95/5), SO_3H HTT 353/27	2.02	1.33	0.02	0.65	0.131
TMOS/BTMB (95/5), SO_3H HTT 368/27	2.35	0.93	0.01	0.72	0.130
TMOS/BTMB (90/10), SO_3H HTT 353/15	3.08	2.09	0.01	2.07	0.647
TMOS/BTMB (90/10), SO_3H HTT 353/27	3.17	1.60	0.00	1.76	0.548
TMOS/BTMB (90/10), SO_3H HTT 368/27	3.97	1.15	0.01	1.04	0.324